Chapter 14

Bulk and In Situ Quantification of Coniferaldehyde Residues in Lignin

Edouard Pesquet, Leonard Blaschek, Junko Takahashi, Masanobu Yamamoto, Antoine Champagne, Nuoendagula, Elena Subbotina, Charilaos Dimotakis, Zoltan Bascik, and Shinya Kajita

Abstract

Lignin is a group of cell wall localised heterophenolic polymers varying in the chemistry of the aromatic and aliphatic parts of its units. The lignin residues common to all vascular plants have an aromatic ring with one *para* hydroxy group and one *meta* methoxy group, also called guaiacyl (G). The terminal function of the aliphatic part of these G units, however, varies from alcohols, which are generally abundant, to aldehydes, which represent a smaller proportion of lignin monomers. The proportions of aldehyde to alcohol G units in lignin are, nevertheless, precisely controlled to respond to environmental and development cues. These G aldehyde to alcohol unit proportions differ between each cell wall layer of each cell type to fine-tune the cell wall biomechanical and physico-chemical properties. To precisely determine changes in lignin composition, we, herein, describe the various methods to detect and quantify the levels and positions of G aldehyde units, also called coniferaldehyde residues, of lignin polymers in ground plant samples as well as in situ in histological cross-sections.

Key words Lignin, Xylem cell types, In situ quantitative chemical imaging, Coniferaldehyde residues, Wiesner test, Raman microspectroscopy, Pyrolysis-GC/MS, Thioacidolysis-GC/MS

1 Introduction

The polyphenolic cell wall polymer lignin is essential to the cellular function and cohesion of vascular plants by providing specific biochemical, biomechanical, and water-repelling properties, such as between the different cell wall layers of each cell type and morphotype in xylem tissues [1]. Lignin is mainly composed of C_6C_3 phenylpropanoid units that can be linked by -C–O–C- ether and -C–C- bonds in between their C_6 aromatic and/or C_3 aliphatic parts depending on their chemical structure (Fig. 1) [2, 3]. Lignin

Javier Agusti (ed.), *Xylem: Methods and Protocols*, Methods in Molecular Biology, vol. 2722,
https://doi.org/10.1007/978-1-0716-3477-6_14,

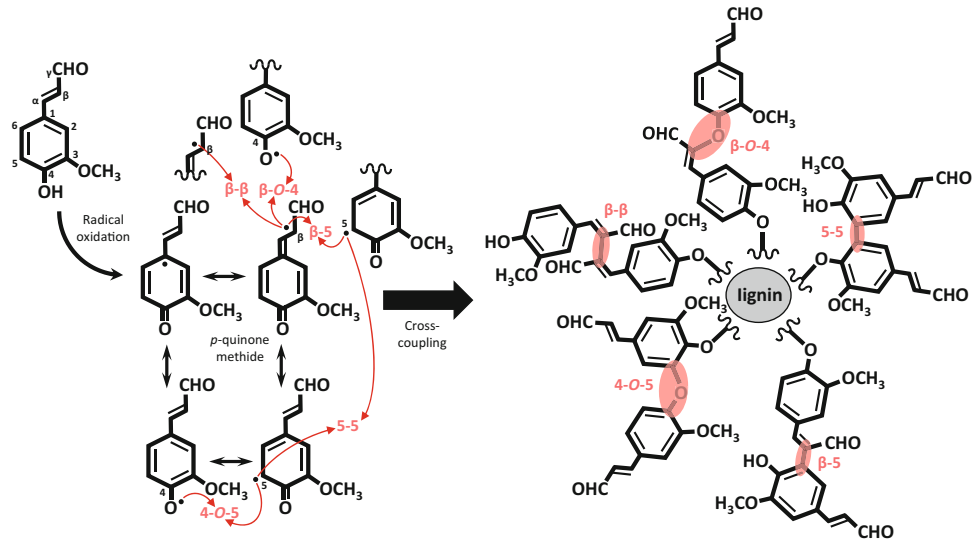

Fig. 1 Coniferaldehyde and inter-unit linkages in lignin polymers. Coniferaldehyde, presenting a C_6 aromatic part with C numbered from 1 to 6 as well as a C_3 aliphatic part with C labelled from α to γ, are oxidized by phenoloxidases and resonate into various mesomers including several *p*-quinone methides that can react with other mesomers to make different linkages between the aromatic and/or aliphatic parts of two monomers. These linkages include uncondensed β-*O*-4 and condensed β-β, β-5, 5–5 and 4-*O*-5 linkages

unit chemistry, thus, varies in their C_6 ring substitution levels with the *para* position baring a hydroxy group and each *meta* positions having either hydrogen, hydroxy, or methoxy groups, as well as in their C_3 terminal aliphatic chain presenting either an alcohol, aldehyde, carboxylic acid, or ester function (Fig. 1) [2, 3]. The accumulation of chemically distinct C_6C_3 residues is conserved between plant species for the different cell wall layers of each cell types [4]. This includes differences in lignin quantities between primary cell walls, cell corners, and secondary cell walls in xylem cells [5, 6], but also differences in chemical composition between xylem cell types with enrichment in mono-*meta* methoxylated C_6 in xylem sap conducting cells (also called guaiacyl or G) compared to enrichment in di-*meta* methoxylated C_6 in xylem fibers (also called syringyl or S) [6, 7]. Compositional specificities also affect the C_3 aliphatic end functions between cell wall layers, G residues including both the very abundant C_3 alcohols, also called coniferyl alcohol units (although the polymerized residues form dihydroconiferyl alcohols), and lower proportions of C_3 aldehyde, also called coniferaldehyde units. In contrast to coniferyl alcohol units abundance in secondary cell walls, coniferaldehyde units accumulate mostly in primary cell walls and cell corners [8] but also differently between cell types and morphotypes, with higher accumulation of coniferaldehyde units in xylem sap conducting cells compared to xylem fibers [6, 7]. These C_3 compositional differences, moreover, vary

during the maturation of each cell types, with G aldehyde units increasing gradually with the maturation of xylem sap conducting cells [1, 6, 9]. Although the majority of lignin residues have alcohol end functions, coniferaldehyde residues represent from 0.1% to 12% of lignin depending on developmental and environmental constraints and plant species [7]. Differences in C_3 end function have huge impact on lignin biochemical, biomechanical, and water-repelling properties depending on the position of the monomer within the polymer: Internal coniferaldehyde units will extend lignin oligo/polymers, whereas coniferyl alcohol units will increase the compactness of lignin [1]. Increases in coniferaldehyde units will also improve cell wall dismantling during digestion [10, 11], increase cell wall water repulsion properties [12], and modify cell wall biomechanics by increasing flexibility but lowering stiffness compared to coniferyl alcohol units [1]. The adjustment of the cell wall properties during the maturation of xylem cells, thus, depends on the precise spatio-temporal accumulation of lignin units with similar C_6 ring substitutions but specific C_3 functions, shifting from more alcohol initially to more aldehyde with aging [1]. As these chemical adjustments vary with cell wall layers, cell types, developmental and environmental conditions for each plant species, precise and reliable methods are needed to estimate these changes. The following article describes the various bulk and in situ methods enabling the precise quantification of coniferaldehyde residues at different position and/or differently linked in lignin polymers from μg to mg amounts for ground samples or at subcellular levels in whole plant biopsies.

2 Materials

2.1 Equipment and Infrastructure

1. Light microscopy:

   Any upright or inverted light microscopes can be used, we have successfully used both an Olympus BX60 upright microscope [1, 6, 11] and a Zeiss Axiovert 200 M inverted microscope [7]. Imaging systems used require a microscope equipped with (i) long-working distance 40x objectives, (ii) a color camera, and (iii) color correction. Additionally, microscope equipped with an automated stage can ease the acquisition of full cross sections. For each used objective, optimize irradiance and gamma correction to fully exploit the dynamic range of the camera. Adjust the red/green/blue correction to represent natural colors. During the experiment, keep those settings constant to facilitate unbiased comparison between samples.

2. Raman microspectroscopy:

   Any Raman microspectrometer can be used, we have successfully used both a Raman Touch-VIS-NIR (Nanophoton, Japan) [1, 11, 13] and a LabRAM HR 800 Raman spectrometer (Horiba, France) [1, 7]. Raman microspectrometry systems require (i) a Nd:YAG laser operating at 532 nm with variable power (0.5–12 mW) and (ii) long-working distance 50x objectives (NA 0.42 to 0.8). Spectrometer parameters included a diffraction grating with 600–1200 grooves mm^{-1} to resolve the spectra. Typically, several hundred scans were accumulated with 1–2 s exposure times from 100 to 2000 cm^{-1} waveband range with a spectral resolution of 1.6–2 cm^{-1}. Note that the optimal parameters (laser power, accumulation number, exposure time) were set to obtain the best quality spectra without causing thermal decomposition of the samples.

3. Gas chromatography and mass spectrometry (GC/MS):

   Any gas chromatography coupled to mass spectrometry (GC/MS) equipment can be used, we have successfully used both a Shimadzu GC-2010 Plus equipped with a HP-5 MS capillary column (30 m × 0.25 mm × 0.25 μm) and a Shimadzu GC/MS QP2020 (Shimadzu, Japan) [1, 11], as well as an Agilent GC/MS 7890A/5975C (Agilent Technologies AB, Sweden) equipped with a pyrolyzer (PY-2020iD or EGA/PY-3030D, Frontier Lab, Japan), and an autosampler (AS-1020E, Frontier Lab, Japan) [1, 6, 7, 11, 13].

2.2 Chemical Solutions

1. Sectioning mounting media

   Mounting media to enable sectioning of plant samples is made of 5–10% (w/v) low-melting point agarose in water. The solution is heated to 70–90 °C using microwave to solubilize the agarose and then kept at 60 °C ready to be added to plant samples.

2. Wiesner test or phloroglucinol/HCl solution:

   Ready-to-use Wiesner test solution is made with 0.5–2% (w/v) phloroglucinol in 1:1 (v/v) 99.5% ethanol: 37%/12.1 M HCl, although lower concentrations of HCl and other acids, such as formic acid, can be used. The solution will turn from translucid to yellow/orange with time, but this color change will not affect staining, background, nor sensitivity. Renewing the solution regularly is recommended, and long-term storage can be made if no acid is added to the ethanolic solution of phloroglucinol (*see* **Note 1**).

3. Solutions for extractive-free cell wall preparation and thioacidolysis:

   Solutions for the cell wall isolation can be prepared and stored long in advance in contrast to solutions for the thioacidolysis, which should be prepared fresh prior to usage,

specifically for the main thioacidolysis solution composed of (v/v/v) 1,4-dioxane:ethanethiol:boron trifluoride diethyl ether (87.5:10:2.5). Note that proper handling of solvents under a chemical hood is necessary for thioacidolysis.

3 Methods

3.1 Producing Synthetic Lignin with Only Coniferaldehyde Units

1. Principles behind synthetic lignin or dehydrogenation polymers (DHPs)

   Dehydrogenation polymers (DHPs) are synthetic lignin polymers made directly in test tubes by co-incubating purified phenoloxidase enzymes, such as peroxidase or laccase, which are capable of radically oxidizing phenolic compounds, with phenylpropanoids of specific chemistry, such as coniferaldehyde monomers, as well as other co-substrates necessary for each type of phenoloxidase (H_2O_2 for peroxidases or O_2 for laccases). The in vitro oxidative polymerization will then occur during the incubation time by the combinatorial cross-coupling of two resonating radical coniferaldehyde monomers (Fig. 1), and the resulting polymer property/structure is fine-tuned by the way/rate coniferaldehyde monomers are supplied to the phenoloxidase: either all at once in a process called *zulauf* [7] or gradually by dripping coniferaldehyde during the incubation time in a process called *zutropf* [13]. Additional factors such as the concentration of phenoloxidase [14], the type of phenoloxidase used [15], and the pH of the reaction buffer [15] can also alter lignin polymer characteristics. DHPs can then be used as references in bulk and in situ analyses [7, 11, 13].

2. Sequential steps to synthesize DHPs

   (a) *Preparing enzyme solution:* Solution of 0.1 mg/mL horseradish peroxidase (HRP) is prepared in 0.1 M sodium phosphate buffer at pH 6 and placed in a 50 mL clean Erlenmeyer flask with a magnetic stirring bar (Fig. 2) (*see* **Note 2**).

   (b) *Preparing substrate and co-substrate solutions:* A 10 mL solution of 12 mM of monomer (coniferaldehyde MW = 178.18 g/mol) is prepared in 3:7 (v/v) methanol:phosphate buffer (0.1 M, pH 6) (*see* **Note 3**) and a 10 mL solution of 14 mM H_2O_2 is prepared in H_2O (*see* **Note 4**).

   (c) *Polymer synthesis:* Polymers are synthetized for 24 h at 25 °C under constant stirring using a magnetic stirrer inside a temperature-controlled cabinet (Fig. 2). For *zulauf* synthesis, all solutions are mixed together and the Erlenmeyer flask is sealed with five layers of parafilm. For

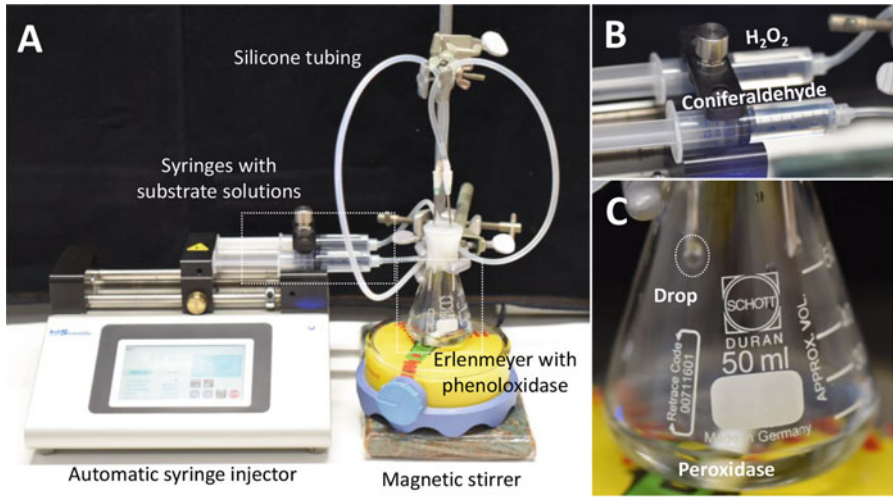

Fig. 2 Set-up for the gradual or *zutropf* synthesis of dehydrogenation polymers (DHP) or synthetic lignins. (**a**) Organisation of the set-up with an automatic syringe injector controlling the rate of drop addition to the HRP enzyme solution in an Erlenmeyer flask under agitation. Note that syringes dispense their content directly into the agitating Erlenmeyer using silicone tubing. (**b**) Close-up on the two syringes with the different substrates to enable the oxidative activity of peroxidases. (**c**) Close-up of Erlenmeyer flask with agitated peroxidase solution. Note that substrates drip as drops in the agitating solution

zutropf synthesis, monomer and H_2O_2 solutions are transferred to 10 mL syringes (Fig. 2), the Erlenmeyer flask with the enzyme solution is sealed with five layers of parafilm, and two silicon tubes (diameter 2–3 mm) are used to connect the end of syringes to a syringe needle piercing the parafilm cap (Fig. 2) (*see* **Note 5**). Dripping of solutions from syringes in the Erlenmeyer is set at the rate of 0.5 mL/h using a Legato 200 syringe pump.

(d) *Polymer purification:* The solution from the 50 mL Erlenmeyer flask is transferred to a 50 mL conical centrifugation tubes. Precipitation is enhanced by adding 150 µL of 12 M HCl and incubating the solution for 30 min at 4 °C. DHPs are then pelleted by centrifugation at 10,000 g using fixed angle rotor. The pellet is then washed with butanol, then twice with ultrapure water, and subsequently freeze-dried.

3.2 Total Coniferaldehyde Unit Quantification in Lignin Using Pyrolysis-GC/MS

1. Principles behind coniferaldehyde unit quantification using pyrolysis

   Pyrolysis enables the thermal degradation of polymers under a limited amount of oxygen, cleaving the weakest links by hemolysis (for C–C and C–O) within lignin polymers and releasing pyrolyzates, mostly phenol-alkenes like coniferaldehyde and coniferyl alcohol residues, independently of the type

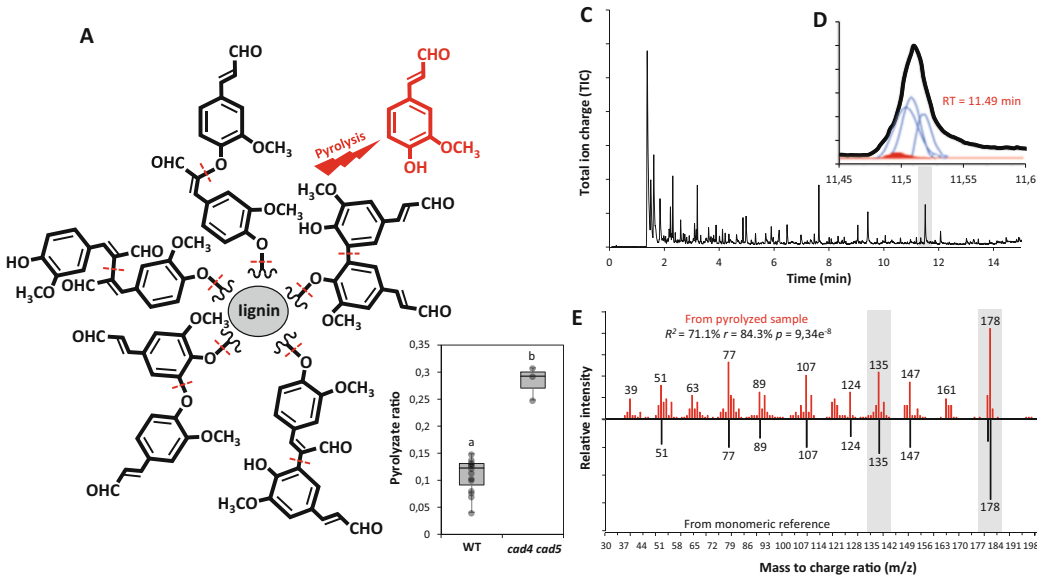

Fig. 3 Pyrolysis-GC/MS for total coniferaldehyde unit quantification in lignin polymers. (**a**) General principle of pyrolysis of lignin polymer through the hemolytic cleavage (shown by dotted red lines) of inter-monomeric linkages to release smaller phenyl-alkene pyrolyzates. (**b**) Relative proportion of coniferaldehyde to coniferyl alcohol unit pyrolyzates from stems of wild-type (WT) and *cad4 cad5* double loss-of-function *Arabidopsis thaliana* plants. Comparison included n = 5–9 independent stem samples through one-way ANOVA with a Tukey-Kramer post hoc test ($\alpha = 0.05$) where significance was presented using different letters. (**c**–**d**) Pyrogram of *Arabidopsis thaliana* WT stems – overall pyrogram is presented in (**c**) and close-up is presented in (**d**) where the different pyrolyzate contributions are deconvoluted (in red coniferaldehyde and in blue coniferyl alcohol). Note that no correction for differences in response factors are made. (**e**) Mass to charge (m/z) fragmentation profile of lignin coniferaldehyde unit pyrolyzate from *Arabidopsis thaliana* stems (in red) compared to reference chemical standards (in black), regression analysis is presented between both profiles as well as key ions shaded in grey for the identification of coniferaldehyde pyrolyzates

of linkage binding them to the polymer (Fig. 3a) [17]. The resulting pyrolyzates are separated using gas chromatography (Fig. 3c, d) and identified with mass spectroscopy – coniferaldehyde residues have specific mass to charge (m/z) signatures with diagnostic 178 and 135 ions (Fig. 3e) [18–21]. The chemical structure of lignin residues from pyrolysis depends on both primary thermal cleavage and secondary thermal reorganization reactions once cleaved when performed in the temperature range of 400–450 °C [17]. Primary pyrolytic cleavage (occurring up to 400 °C) enables the release from lignin of G residues with unsaturated alkyl groups, like coniferaldehyde residues. Additional chemical processes such as oxidation/reduction of alcohols into aldehydes will also occur at low pyrolysis temperature (around 250 °C) but not at higher temperature [17]. Secondary pyrolytic reorganisation (from 400 to 450 °C) can then alter the chemical structure of pyrolyzates by

either demethylating aromatic groups and/or shortening the length of aliphatic chains, leading to the increased release of the G benzaldehyde called vanillin. Coniferaldehyde residues released from the pyrolysis of lignin at high temperature, thus, include mostly *bona fide* coniferaldehyde units freed from primary pyrolysis of lignin but also some unspecific products derived from the oxidation of the terminal aliphatic function of coniferyl alcohols [17]. High temperatures ~450 °C and rapid pyrolysis of several seconds are, thus, recommended to limit the formation of unspecific products and enable the release of *bona fide* lignin fragments. Coniferaldehyde residues can thus be accurately measured and compared in plant samples of different genotypes, such as between *Arabidopsis thaliana* stems of wild-type (WT) and loss-of-function in *CINNAMYL ALCOHOL DEHYDROGENASEs* (*CAD*) *4* and *5*, blocking the conversion of coniferaldehyde into coniferyl alcohol monomers (Fig. 3b) [7, 11]. Pyrolysis-GC/MS, thus, represents a rapid micro-scaled method to accurately estimate changes in the proportion of total coniferaldehyde residues in lignin polymers.

2. Sequential steps to perform pyrolysis-GC/MS analyses
   (a) Frozen samples are first freeze dried, using for example a ScanVac CoolSafe Pro110-4 (LABOGENE, Denmark) freeze drier, for at least overnight, to ensure to removal of any residual water (*see* **Note 6**).
   (b) Freeze-dried samples are then ball-milled to reach diameter of fine particle below ca. 300 μm. For soft materials like *Arabidopsis* stems, samples are placed in 1.5 mL metal small jars with 1 small bead of 7 mm diameter and milled at 30 Hz for 1–2 min in a standard ball mill (such as Retsch MM400). Hard materials like poplar wood are preferably first fragmented into smaller fragment of around 500 μm, using a centrifugal mill (such as Retsch ZM200), and then placed in 10 mL metal containers with a large metal bead (13 mm diameter) and milled at 30 Hz for 1–2 min in a standard ball mill (*see* **Note 7**).
   (c) About 50–70 μg (optimally 60 μg) of milled plant sample are weighted using a microbalance and aliquoted into a pyrolysis cup. Each aliquot is then stored in a 96-well plate in a desiccator until pyrolysis.
3. Pyrolysis of samples and analysis of pyrograms

   Aliquoted ball-milled samples are delivered to a pyrolyzer equipped with an auto sampler connected to a GC/MS, as described in Subheading 2.1, item 3. After 20 sec of pyrolysis at 450 °C, pyrolysates are separated on a J&W DB-5MS

capillary column (30 m length, 0.25 mm diameter, 0.25 μm film thickness). The following oven program is used for the chromatographic separation: 40 °C, followed by a temperature increase of 32 °C/min to 100 °C, then 6 °C/min to 120 °C, then 15 °C/min to 250 °C, and, finally, 32 °C/min to 320 °C, which was kept for additional 3 min. The total run time is 19 min, and scanned spectra were recorded in the range 35–250 m/z [18]. Pyrograms are then analyzed by any analytical software, such as OpenChrom (http://www.openchrom.net/), to identify each pyrolyzate based on their m/z and retention time. R can also be used to deconvolute the contribution of each pyrolyzate in the pyrogram, enabling one to determine the contribution of each overlapping pyrolyzate peak, such as the ones between coniferaldehyde and coniferyl alcohol residues in lignin (Fig. 3d) [18]. The proportion of each pyrolyzate is then expressed as percentage of the overall pyrogram, the sum of the pyrolyzates with phenolic rings or compared to other pyrolyzates with the same phenolic ring substitution (Fig. 3b) (*see* **Note 8**).

3.3 Terminal and Internal Ether-Linked Coniferaldehyde Unit Quantification in Lignin Using Thioacidolysis-GC/MS

1. Principles behind coniferaldehyde unit quantification using thioacidolysis

   Thioacidolysis restrictively cleaves glycerol aryl ether linkages in between the C_6 *para* hydroxy group of one lignin unit and the C_3 β carbon of another, known as β-*O*-4 (Fig. 1). The detailed chemical reactions enabling the β-*O*-4 cleavage of coniferaldehyde units in lignin using thioacidolysis is presented in Fig. 4. Depending on the position of coniferaldehyde units in the lignin polymer, thioacidolysis products will lead to either thioethylated products for terminal residues with free aliphatic part (terminal residues with free aliphatic part linked only by one β-*O*-4, labeled A in Fig. 4) or indenes for internal and terminal residues with free aromatic part (internal residues interlinked by two β-*O*-4 and terminal residues with free aromatic part linked by one β-*O*-4, labeled B in Fig. 4) (*see* **Note 9**). Both trithioketals and indene dithioketals have distinct retention times (Fig. 5a, b) and specific mass spectrum, enabling their clear identification (Fig. 5e, g). Representative yields in *Arabidopsis* and poplar always show detectable amounts of terminal thioethylated products (representing between 1% and 2% of the total chromatogram area) in all genotypes tested [7], but indenes are less abundant and mostly accumulated in knock-out or knock-down plants in *CINNAMYL ALCOHOL DEHYDROGENASEs* (*CADs*) [11]. Internal coniferaldehyde thioacidolised products, moreover, result in two regioisomers with the int.1 form 8–10 fold more abundant than int.2 form in both poplar and *Arabidopsis* (Fig. 5c) [22]. Comparison between stems of *Arabidopsis* wild-type

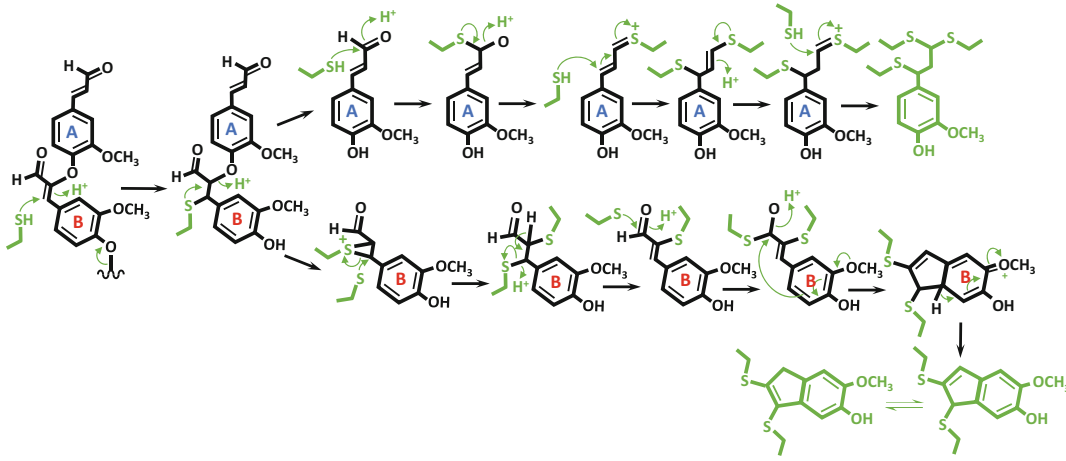

Fig. 4 Schematic representation of the chemical reactions behind the thioacidolysis of β-*O*-4 linked coniferaldehyde residues depending on their position in lignin polymers. Two coniferaldehyde units are presented linked by β-*O*-4 with one in terminal position with a free aliphatic chain (labelled A) and another internal or terminal with a free aromatic ring (labelled B). Sequential reactions occurring during thioacidolysis produce distinct thioethylated products depending on the position of coniferaldehyde monomers in the lignin polymers – one thioethylated product for terminal residues with free aliphatic chain and two regioisomeric indenes for internal or terminal residues with free aromatic ring. *See* references [22, 27, 28]

(WT) and loss-of-function in *CAD4* and *5*, named *cad4 cad5* [1, 11], illustrates differences in both coniferaldehyde residue content and changes of coniferaldehyde unit position in lignin polymers between genotypes (Fig. 5d). Thioacidolysis-GC/MS represents a highly reliable milli-scaled method to accurately estimate the proportion and position of β-*O*-4-linked coniferaldehyde units in lignin polymers.

2. Preparation of extractive-free cell wall material

   Extract-free cell wall materials are isolated from plant samples ground in liquid nitrogen using ceramic mortar and pestle and then transferred using spatula to fill half of 2 mL sterile microtubes. Samples are then sequentially treated with 1 mL of solutions, vortex mixed for 15–20 sec, and cell wall isolates pelleted with centrifugation (10,000 g, 10 min) to discard the supernatant removing (i) first proteins with three washes of 140 mM Tris-base, 105 mM Tris-acetate, 0.5 mM ethylenediamine tetraacetic acid, and 8% w/v lithium dodecyl sulfate; (ii) then two washes of water; (iii) two washes of 100% methanol; (iv) one wash of chloroform:methanol (1:1); and, finally, (v) one wash of acetone. Pellets are then air-dried overnight.

3. Sequential steps to perform thioacidolysis

   (a) Dried isolated extractive-free cell walls are weighted and 5–10 mg are transferred to a 1 mL vial. Internal standard

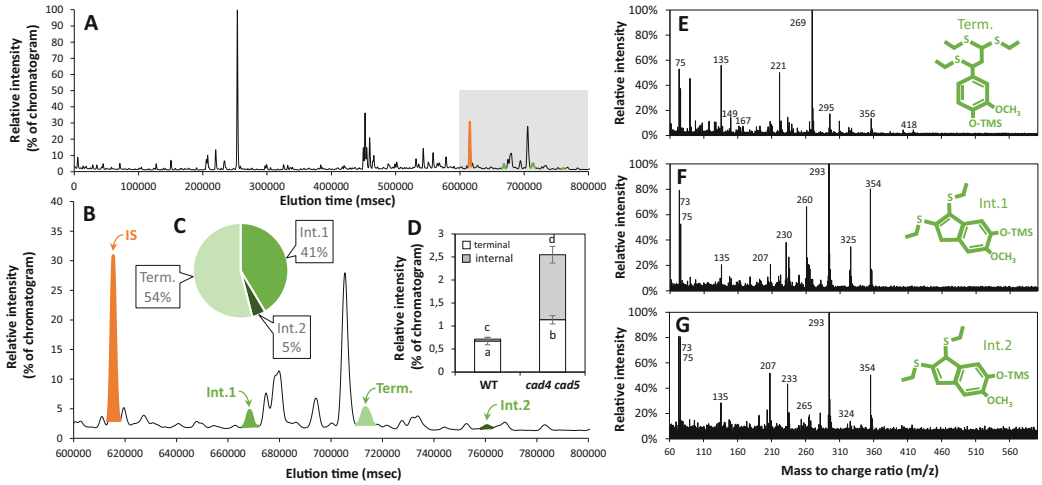

Fig. 5 Thioacidolysis of β-*O*-4 linked coniferaldehyde residues in lignin polymers. (**a**–**b**) Gas chromatogram of the thioacidolyis products of lignin including internal standard (IS in orange - tetracosane) and coniferaldehyde thioacidolysed products (in green) – overall chromotagram is presented in (**a**) and close-up is presented in (**b**) where each thioacidolysis product is clearly separated. (**c**) Relative proportion of the summed chromatogram area comprised by the different thioacidolysis products of coniferaldehyde. Note that similar response factors have been assumed between these thioacidolysed products. (**d**) Relative proportion of the different coniferaldehydes in stem thioacidolysed products for terminal and internal monomers in wild-type (WT) and *cad4 cad5* double loss-of-function *Arabidopsis thaliana* plants. Comparison included n = 3–4 independent stem samples through one-way ANOVA with a Tukey-Kramer post hoc test ($\alpha = 0.05$) where significance was presented using different letters. (**e**–**g**) Mass to charge (m/z) fragmentation profiles of the different thioacidolysed products of coniferaldehyde depending on their position in lignin with terminal (Term.) producing thioethylated product (**e**) and internal (Int.) producing two types of indene regioisomers (**f-g**)

tetracosane (100 µg, 10 µL of 10 mg/mL) is then added to each sample, and the vials are dried overnight with a vacuum pump.

(b) Total 800 µL of (v/v/v) 1,4-dioxane: ethanethiol: boron trifluoride diethyl ether complex (87.5:10:2.5) are added to each vial, which are then closed and tightened using screw-on caps and sealed with Teflon tape.

(c) Vials are mixed using strong vortexing for 10–20 sec, wrapped in aluminum foil and heated at 100 °C for 4 h in a sand bath (*see* **Note 10**).

(d) Vials are removed from the sand bath and cooled on ice for several minutes.

(e) Total 200 µL of the sample solution are then transferred to a 1.5 mL microtube, supplemented with 100 µL of 1 M sodium bicarbonate in water, mixed by vortexing, and then centrifuged for 2–5 sec using a benchtop minicentrifuge.

(f) Total 130 μL of 1 M hydrochloric acid are then added to adjust the pH of the solution to 3–4 (checked using pH-test paper).

(g) About 250 μL of diethyl ether are added, and the solution is mixed by vortexing and then centrifuged for 10–30 sec using a benchtop minicentrifuge to separate aqueous and organic phases. The upper organic phase is then transferred to a new microtube. This step is repeated three times to ensure that all of the thioacidolysed products are recovered.

(h) About 100 μL of saturated saline solution is added to the organic phase, mixed by vortexing and centrifuged. The upper phase is then transferred to a new 1.5 mL microtube containing 100–150 mg sodium sulfate. The new solution is then mixed by vortexing and centrifuged briefly using a benchtop minicentrifuge.

(i) Samples are then transferred to a 1 mL vial, air dried with a nitrogen stream, then closed and tighten using screw-on caps and stored at −20 °C until analysis (*see* **Note 11**).

4. Chromatographic analyses of thioacidolysis

About 250 μL of diethyl ether are added to each vial, vortexed and left to stand on the bench for at least 5 min. Then 10 μL of the supernatant is transferred to an insert in a GC vial and supplemented with 50 μL of N,O- Bis (trimethylsilyl)trifluoroacetamide and 50 μL of anhydrous pyridine, then heated at 60 °C for 1 h. Finally, 100 μL of dichloromethane is added and mixed thoroughly, and the vial is closed and placed in the GC autosampler for analysis. The remaining part of the samples are dried again and stored at −20 °C. Chromatographic analysis is performed on a standard GC/MS, as described in Subheading 2.1, **step 3**, with an injector at 250 °C. The column temperature program used include 60 °C (2 min), from 60 to 260 °C (15 °C min^{-1}), 260 °C (18 min), from 260 to 300 °C (5 °C min^{-1}), and 300 °C (10 min). Mobile phase used helium at a rate of 1.46 mL/min. Chromatograms are finally analyzed by any analytical software, such as OpenChrom (http://www.openchrom.net/), to identify each trimethylsilyl (TMS) thioacidolysed product based on their retention time and m/z profile, and to quantify their contribution to the total chromatogram peak area normalized by the internal standard tetracosane (Fig. 5).

3.4 Total Coniferaldehyde Unit Quantification in Lignin In Situ Using the Wiesner Test

1. Principles behind coniferaldehyde unit quantification using Wiesner test

Probably the oldest and most used histochemical test in plant sciences, the Wiesner test enables the quantitative chemical imaging of total coniferaldehyde units in lignin with

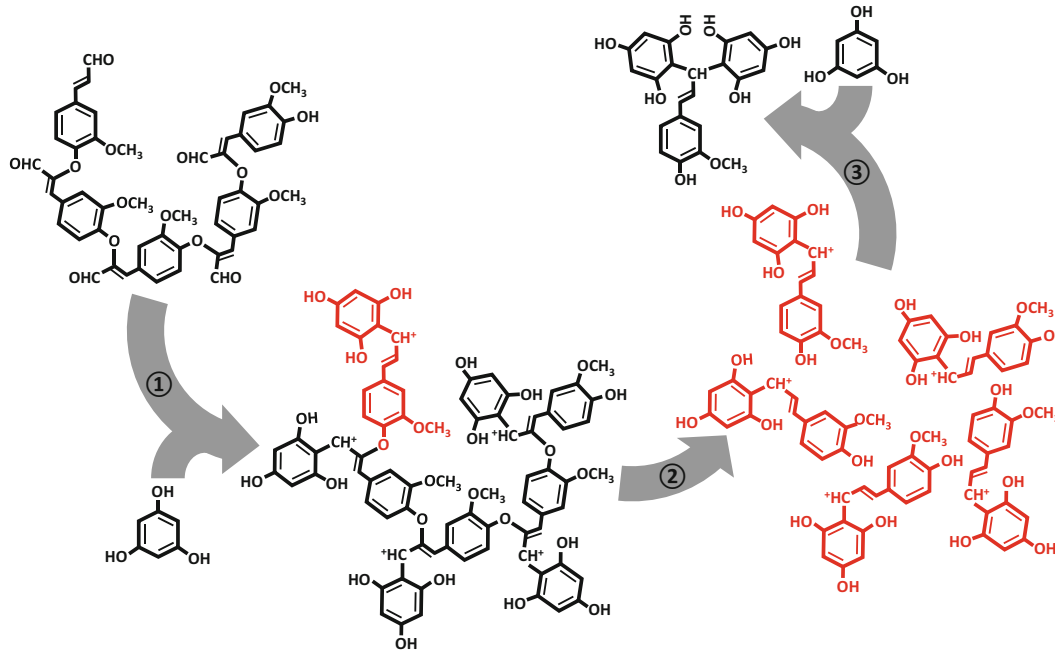

Fig. 6 Schematic representation of the sequential chemical reactions behind the Wiesner test for coniferaldehyde unit quantification in lignin. The Wiesner test sequentially reacts with the coniferaldehyde units of lignin independently of their position in the polymer by (1) forming mono-phloroglucinol conjugate carbocations in acidic conditions where only terminal residue exhibit chromogenic activity, followed by (2) the gradual fragmentation through ethanoacidolysis of lignin polymers into smaller fragments that proportionally free more terminal mono-phloroglucinol conjugates with chromogenic activity, and finally leading (3) to a second conjugation with another phloroglucinol in acidic conditions to form di-phloroglucinol conjugates that are not chromogenic

subcellular resolution levels [7, 11]. The Wiesner test staining chemical reactions occur sequentially with (i) acid-dependent conjugation of coniferaldehydes with phloroglucinol into monophloroglucinol-coniferaldehyde carbocations, which are chromogenic in low pH; (ii) ethanoacidolysis of lignin polymers into shorter oligo/monomers, enabling internal conjugates to become terminal; and (iii) a second acid-dependent conjugation with phloroglucinol, forming diphloroglucinol-coniferaldehyde conjugates that are not chromogenic (Fig. 6). The monophloroglucinol-coniferaldehyde carbocations resonate in acid conditions to produce a chromogene absorbing at λ of 547 nm with a red to purple hue (Fig. 7a–c). The staining reaches its peak after 5–15 min when it releases all the terminal monophloroglucinol-coniferaldehyde conjugates during the ethanoacidolysis (Fig. 7d, e) and faints afterward as diphloroglucinol-coniferaldehyde conjugates form [7, 22, 23]. The intensity and sensitivity of the Wiesner test chromogenic reaction depends both on the local levels of

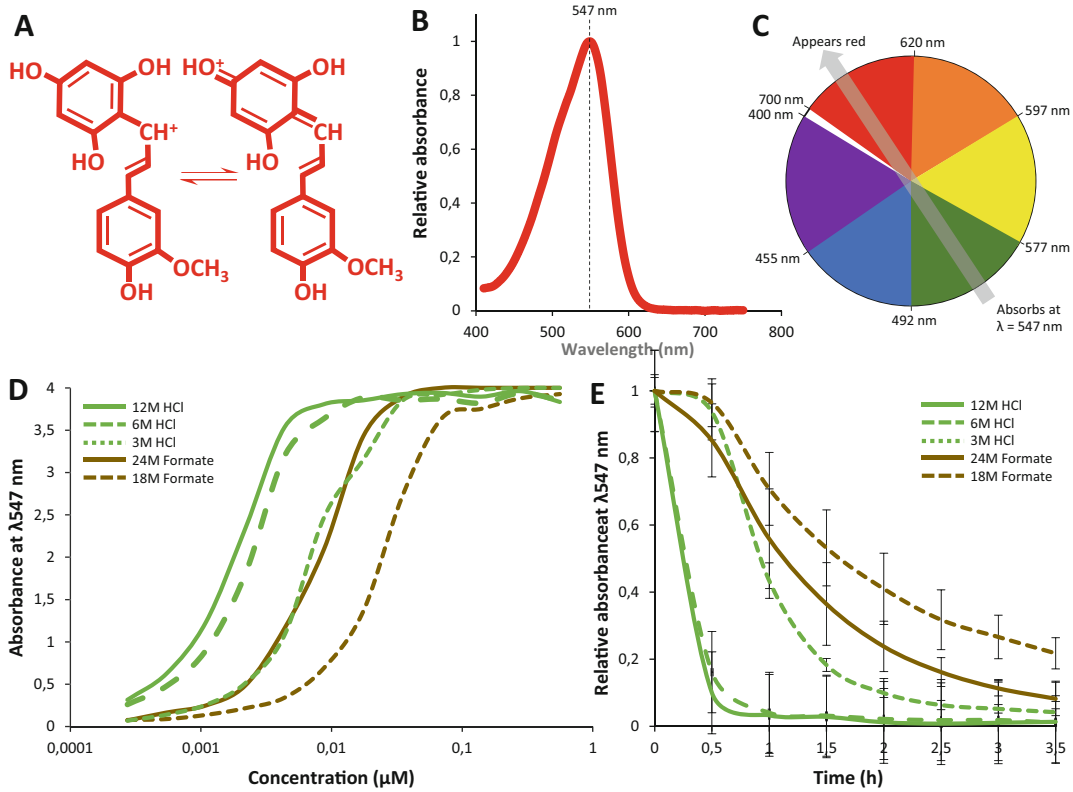

Fig. 7 Identity, absorbance and stability of the Wiesner test chromophore. (**a**) Mesomeric resonance forms of the chromogenic mono-phloroglucinol conjugate carbocations of the Wiesner test. (**b**) UV-Vis absorbance spectra of the Wiesner test mono-phloroglucinol conjugate carbocations in acidic conditions with a single maximum absorbance peaking at 547 nm. (**c**) Color wheel representation of the chromophore color based on its absorbance maximum. (**d**) Effect of the 1 volume acid concentration added to the 2% phloroglucinol ethanol solution for the formation of mono-phloroglucinol conjugate carbocations and its quantitative relationship with coniferaldehyde concentration. Note that 1 volume of 24 M formic acid resulted in similar detection sensitivity than 1 volume of 3 M HCl. (**e**) Effect of the 1 volume acid concentration added on the lifetime of mono-phloroglucinol conjugate carbocations. Note that strong acid condition with 12 or 6 M HCl cause rapid conversion into di-phloroglucinol conjugates

coniferaldehyde units in lignin and on the pH of the solution (Fig. 7d, e). Although the Wiesner test is also often called phloroglucinol/HCl, other acids, such as formic acid, can be used to reach similar intensity and sensitivity (Fig. 7d, e). The Wiesner test, thus, represents a rapid and highly reliable method to accurately estimate the total coniferaldehyde unit content in lignin polymers with subcellular resolutions in plant histological samples.

2. Mounting samples and imaging

   (a) *Sample preparation and sectioning:* Cellular content, interfering pigments and extractives are removed by incubating plant samples in 70% ethanol for several days before

staining [6, 7]. Samples are then embedded in warm 5–10% agarose, described in Subheading 2.2, **step 1**, using the cap of 1.5 or 2 mL microtubes as a cast support. Samples are first oriented vertically in the warm agarose and then left on the bench to settle for 10–15 min. Solidified agarose plugs with embedded samples are then removed from their cast support with tweezers, glued using ethylcyanoacrylate (ECA) glue onto the sample holder of a vibratome (such as a Leica VT1000S), and the glue is left to set for 10–15 min. The sample holder is then mounted in the vibratome and the sectioning tray filled with distilled water to cover the agarose plug. Sectioning parameters to make 50 μm histological cross sections are performed at a speed of 0.20 mm/s (4 on the speed dial), 70 Hz frequency (7 on the frequency dial), with half of a razor blade tilted at ~5° from the horizontal (using angle level in blade mounting bracket). These parameters should be adjusted by the user to the properties of each plant sample depending on its hardness and size.

(b) *Sample imaging:* 50 μm thick cross sections from cleared plant samples are imaged between 1 mm thick glass slide and 150 μm thick coverslip before staining in water only and after staining just a few minutes after adding 40–50 μL of Wiesner test solution (Fig. 8). Acid concentration can be lowered or replaced by weaker acids, but this will both lower the detection sensitivity and increase the chromogene lifetime (Fig. 7d, e). The removal of the coverslip after imaging the unstained sample can lead to damages, leaving a nonoverlapping portion of the coverslip over the microscopy slide to grab with tweezers will ease the removal of the coverslip and reduce damages. Imaging is performed using standard brightfield microscopes, as described in Subheading 2.2, **step 2** [6, 7].

(c) *Image processing prior to analysis:* All image handlings are made using open-source image analysis software Fiji/ImageJ [24–26].

  (i) *Image correction for uneven illumination:* If necessary, uneven background illumination during image acquisition is corrected by first taking an image of an empty area of the glass slide and cover slip with identical illumination and acquisition parameters. This image is then subtracted from a plain white image using the Fiji image calculator (in "Process/Image Calculator…" tab, and selecting images and using the operation "subtract"). The result of this subtraction can then, again using the image calculator, be added to the images of samples, resulting in an evenly white background between images.

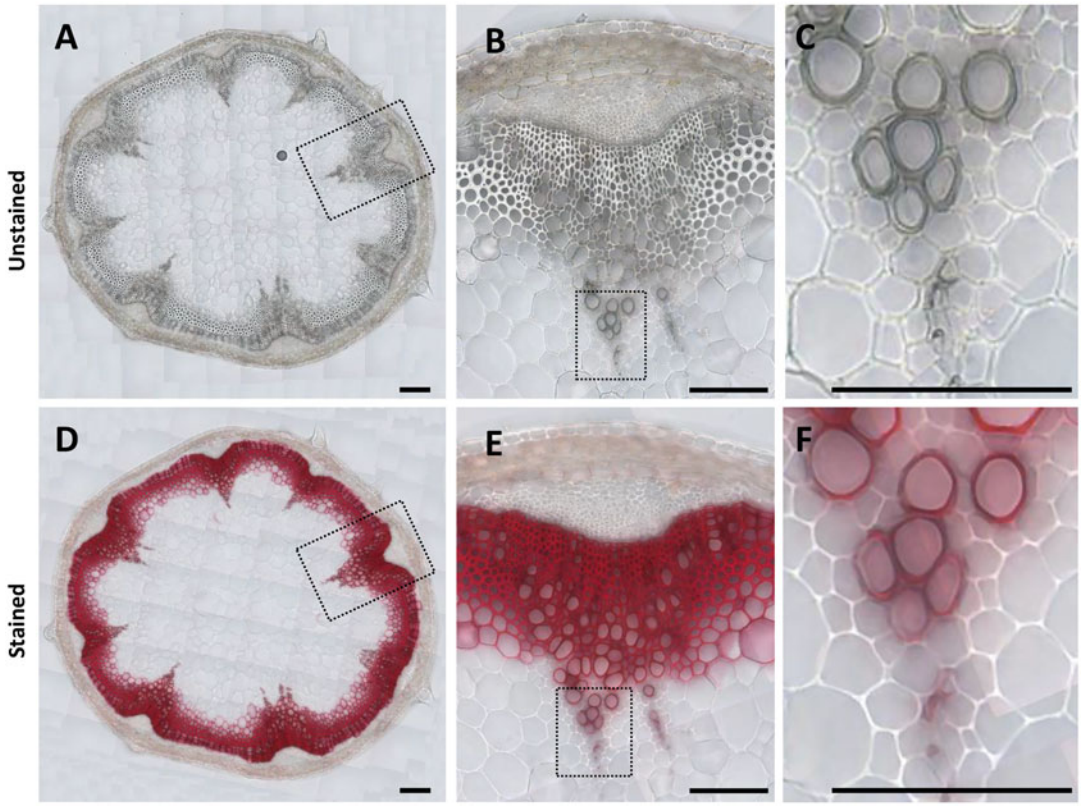

Fig. 8 Wiesner test staining of coniferaldehyde in whole plant cross-sections assembled using image stitching with 10% overlaps. (**a**–**c**) Unstained stem cross-sections of *Arabidopsis thaliana* WT prior to the Wiesner test staining observed as a whole (**a**), close-up of vascular bundle (**b**) and meta- and proto-xylem vessels (**c**), bars = 75 μm. (**d**-**f**) Stained stem cross-sections of *Arabidopsis thaliana* WT after 3 min of Wiesner test staining observed as a whole (**d**), close-up of vascular bundle (**e**) and meta- and proto-xylem vessels (**f**), bars = 75 μm

(ii) *Stitching images together to form full sections:* Overlapping images of a larger sample (background corrected if necessary) can be stitched together into a larger image (Fig. 8) using the "Grid/Collection stitching" plugin [24]. Images need to be acquired with at least a 10% overlap between each other to enable proper stitching. Increasing the overlap can, moreover, improve the probability of successful stitching.

(iii) *Assembling and aligning RGB image stack:* Images (single images or stitched mosaics) of the same sample before and after staining are then assembled into a stack of images using the "Image/Stack" tab and selecting "Images to stack." Make sure that the unstained and stained images have the same

dimensions in pixels; otherwise, use the "Image/Scale" tab to adjust image size. Finally, the stacked images are aligned to each other using image registration, such as the "Linear Stack Alignment with SIFT" plugin. If the alignment is not satisfactory, possibilities for troubleshooting are using the "bUnwarpJ alignment" plugin or cutting the images to a smaller sizes before aligning.

(d) *Processed image analysis:* Wiesner test signal measurements include determining (i) the hue of unstained and/or stained region-of-interest (ROI) by converting the RGB image stack into the hue/saturation/brightness (HSB) color space and (ii) the optical density or absorbance of unstained and/or stained ROIs by converting the RGB image stack into 8-bit image stack. To ease the understanding of the image processing steps, both color and intensity scales have been added to Figs. 9 and 10 below each image and submitted to the same image conversion steps to show how each image is affected and how reproducible measurements are obtained. The measured areas are either defined by ROIs using "Oval" or the "Line" selection tools of ImageJ that are drawn at specific positions in the aligned image stack, and then measured using "Analyze/measure" for "Oval" ROIs to obtain average, median, area, minimal and maximum values (defined using "Analyze/Set Measurements...") or using "Analyze/Plot profile" for "Line" ROIs to obtain y values along the x distance (data is obtained using "Data >> Copy all data").

(i) *Measuring hue:* Hue measurements are obtained by transforming the aligned images stacks from the RGB into the HSB color space. This conversion is made using the "Image/Adjust" tab and selecting "HSB," which will convert each single RGB image into an image stack of three distinct images for hue, saturation, and brightness (Fig. 9). Note that hue, saturation, and brightness images will still be in an 8-bit scale. The hue values are obtained using the hue image of the HSB stack. The average hue values on 8-bit scale (ranging from 0 to 255), measured by the ROIs, are then divided by 255 and multiplied by 360 to have the hue degree values of the hue scale (ranging from 0° to 360°). Changes in hue due to Wiesner staining for specific cell types or cell wall layer can, thus, be reliably measured and statistically tested (Fig. 9). Measure single pixels, not ROIs, to avoid the averaging of pixels with 8-bit values close to 0 or

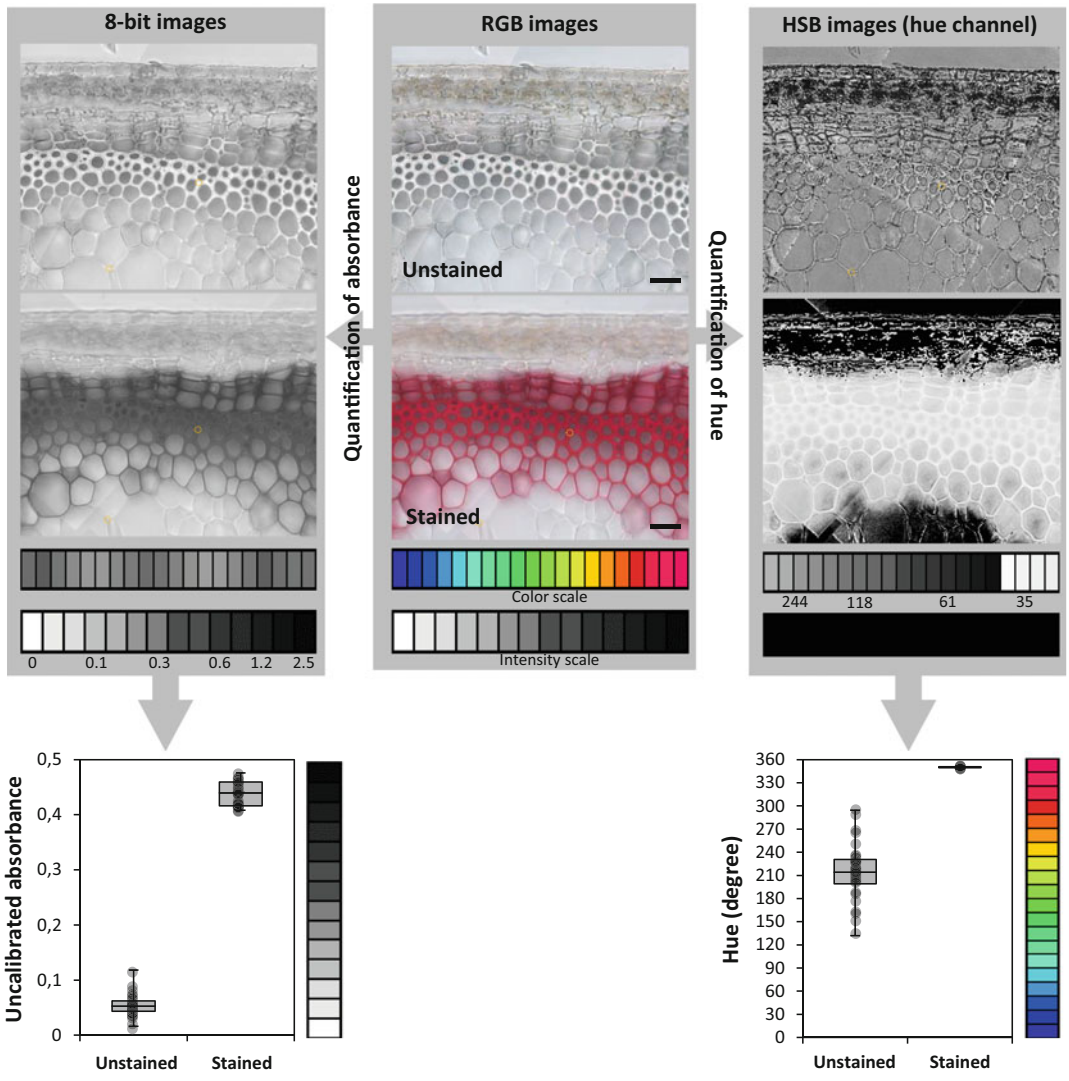

Fig. 9 Determination of Wiesner test absorbance and hue using oval region-of-interests (ROIs). Different image processings lead to different parameters that can be quantified. Two scales, one color scale and another grey-scale intensity, are also presented below each images to show the impact of each image conversion step. For absorbance measurements, images from the initial RGB images (color images in the center of the figure, bars = 50μm) before and after staining are converted in 8-bit scale (left hand side that only affects the intensity and neglects the color) and converted in "uncalibrated absorbance" to show difference in absorbance for the same position of oval ROIs (red dotted circles) between unstained and stained cell walls of interfascicular fibers of *Arabidopsis thaliana* stems. For hue measurements, images from the initial RGB images before and after staining are converted in HSB (left hand side that only affects the color as hue and neglects the intensity) and converted to a hue degree scale to show color differences for the same position of oval ROIs between unstained and stained cell walls of interfascicular fibers of *Arabidopsis thaliana*

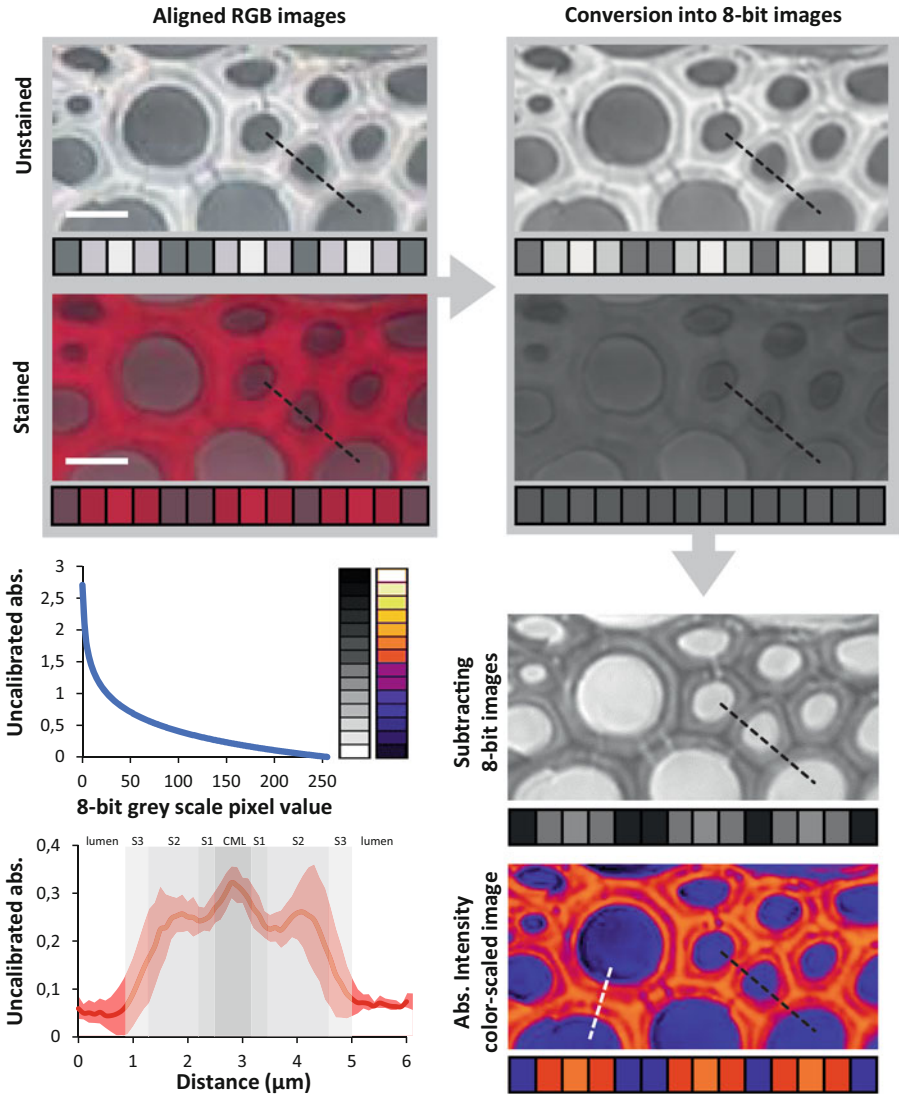

Fig. 10 Image processing and determination of Wiesner test absorbance using line profiles across cell walls to monitor changes between layers. The sequential image processing steps are presented using boxed arrows from the initial RGB images (bars = 8 µm) before and after staining (as well as their schematic representation in boxes showing changes along the segmented black lines), which are then converted into 8-bit scale, then subtracted using "Image Calculator" and converted into artificial intensity color using the "Fire" on "Image/ Look-up tables". Absorbance are obtained by converting the 8-bit subtracted image in "uncalibrated absorbance" (and the exponential relationship between 8-bit and absorbance is presented) and then using line profiles (such as the segmented white line) to determine the change in absorbance across cell wall layers between two neighboring interfascicular fibers of *Arabidopsis thaliana d*

255. As both 0 and 255 are shades of red on the circular hue scale (around 360°), their average on the linear 8-bit scale results in shades of green hue (around 127.5 or 180°).

(ii) *Measuring absorbance:* Unlike in fluorescence images, the intensity in bright field microscopy RGB images is not linearly but exponentially proportional to the pixel value (Fig. 10). To transform pixel values into an approximation of absorbance (still referred to optical density or OD, although nowadays the use of this term is discouraged), the "calibration" function of ImageJ/Fiji is used. The RGB aligned image stack is converted into 8-bit image stack using the "Image/Adjust" tab and selecting "8-bit." Subtracting the aligned unstained image from its corresponding stained image using the "Process/Image Calculator…" tab will enable to obtain the Wiesner test absorbance independently of the background (Fig. 10) (*see* **Note 12**). The 8-bit grey scale values are then converted into absorbance by using the "Analyze/Calibrate..." tab and selecting "Uncalibrated OD." The image will not change visually, but any pixel value measured will change from grey scale intensity to absorbance, which have an exponential relationship (Fig. 10). The absorbance of unstained and stained areas can then be measured using oval ROIs for fixed cell type position (Fig. 9) or between the different cell wall layers of neighboring cells using line ROIs (Fig. 10) (*see* **Note 13**). Changes in absorbance due to Wiesner staining for specific cell types or cell wall layers can, thus, be reliably measured and statistically tested (Figs. 9 and 10).

3.5 Terminal Coniferaldehyde Unit Quantification in Lignin In Situ Using Raman Spectroscopy

1. Principles behind coniferaldehyde unit quantification using Raman spectroscopy

Raman microspectroscopy is a microscopy-based method using Raman scattering or the inelastic scattering of photons from a monochromatic laser at 766 or 1064 nm by the molecular vibrations, varying with linkages and elemental composition of each molecules, and leading to scattered photon with energy shifted up or down, also called a Raman waveband shift (Fig. 11a). The relative scattering intensity of each Raman band shift depends on the chemistry of the compound, the solvent, the spatial orientation of the molecule, and its conformational degree of freedom (Fig. 11c) [11, 13]. Raman microspectroscopy thus enables to discriminate between the chemistry as well as the position of specific monomers in lignin compared to

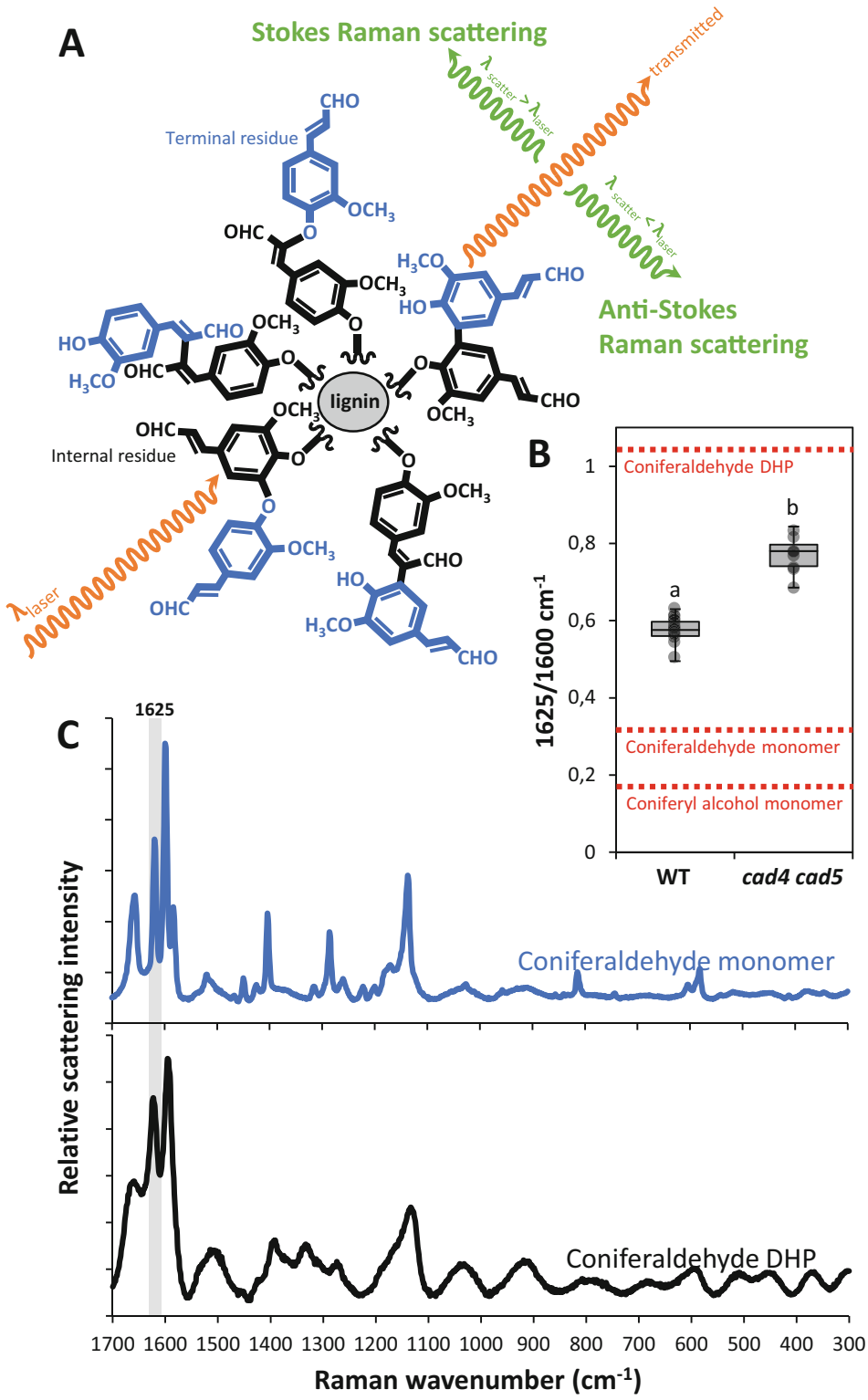

Fig. 11 Determination of coniferaldehyde unit content in cross-section using Raman microspectroscopy. (**a**) Schematic principle of Raman scattering in lignin polymers where coniferaldehyde units have both different position (blue terminal and black internal) and inter-monomeric linkage types. The Raman effect is

other cell wall components made of polysaccharides [1, 6, 13]. The semi-quantitative capacity of Raman spectroscopy for lignin levels and part of its chemistry are now well-established [1, 6, 7, 11, 13], and coniferaldehyde units with free aliphatic chain in terminal positions in lignin polymers can be easily measured using the 1625 cm^{-1} Raman waveband [1, 6, 11, 13]. Comparison between xylem sap conducting cells of *Arabidopsis* wild-type (WT) and loss-of-function in *CAD4* and *5* illustrates differences in terminal coniferaldehyde unit content in lignin polymers in situ compared to synthetic polymers made only of coniferaldehyde units and isolated coniferaldehyde and coniferyl alcohol monomers (Fig. 11a). Raman microspectroscopy, thus, represents a rapid and highly reliable method to accurately estimate the terminal coniferaldehyde unit content in lignin polymers at subcellular resolutions in plant histological samples. Samples can be then processed using the Wiesner test to estimate total coniferaldehyde residue content in lignin to determine relative terminal to total coniferaldehyde unit content with subcellular resolutions [1, 6, 11].

2. Mounting samples and imaging
   (a) *Calibration of spectrometer to silicon standard:* Ensure that the Raman microspectrometer is calibrated with crystalline silicon standard (main waveband at 520 cm^{-1}) prior to acquisition of plant samples.
   (b) *Sample imaging:* 50 μm thick cross sections from cleared plant samples are prepared, as described in Subheading 3.4, **step 2a**, and imaged in water between 1 mm thick glass slide and 150 μm thick coverslip. Imaging at high laser intensity will cause the mounting water to evaporate quickly therefore requiring to top up samples with water between acquisitions.
3. Spectral processing (baseline correction and normalization)
   The acquired Raman spectra are first baseline corrected using an asymmetric least squares algorithm available in the

Fig. 11 (continued) schematized by the photons of a monochromatic laser (wavy orange lines of specific wavelength λ_{laser}) being scattered to higher or lower wavelengths (wavy green lines of λ different than λ_{laser}). (**b**) Relative ration of 1625 cm^{-1} (for coniferaldehyde) to 1603 cm^{-1} (for G type lignin) in lignin in situ of sap conducting cells from stem cross-sections of wild-type (WT) and *cad4 cad5* double loss-of-function *Arabidopsis thaliana* plants. Comparison included $n = 7–12$ independent cells from multiple plants through one-way ANOVA with a Tukey-Kramer post hoc test ($\alpha = 0.05$) where significance was presented using different letters. Note that dotted red lines are added to show 1625 cm^{-1} to 1603 cm^{-1} ratios of DHPs made only of coniferaldehyde as well as coniferaldehyde and coniferyl alcohol monomers. (**c**) Raman scattering spectra of coniferaldehyde as monomer (in blue) or incorporated in homopolymers as DHPs (in black) with the common characteristic 1625 cm^{-1} Raman waveband

"baseline" R package with the following parameters: smoothness $\lambda = 100{,}000$ and asymmetry $p = 0.01$. Differences can be readily observed in the Raman scattering spectra between isolated monomers and their polymerized forms, thus confirming that the position and interlinkage type both affect the Raman scattering of coniferaldehyde units (Fig. 11c). The baseline corrected spectra can then be normalized and analyzed differently:

Normalisation to the area under the curve (AUC): This normalization determines the proportion that each Raman band represents in the overall Raman scattering spectrum of the sample and, thus, postulates that the Raman scattering spectra is proportional to its cell wall polymer content/composition [13]. The AUC of the entire Raman scattering spectra is, thus, first determined between 300–1700 cm^{-1} after baseline correction and the coniferaldehyde unit proportion is determined by dividing the 1625 cm^{-1} band intensities by the AUC.

Ratios to either lignin ~1600 cm^{-1} or cellulose ~380 cm^{-1} wavebands: This normalization determines the ratio of each Raman band relatively to a reference Raman waveband in the sample and, thus, determines ratios of Raman scattering bands that are proportionally dependent on cell wall polymer content/composition [6, 13]. The intensities of the 1625 cm^{-1} band in spectra are, thus, divided by a reference band in the same spectrum either the lignin 1603 cm^{-1} band (Fig. 11b) [13] or by the cellulose 378 cm^{-1} [6].

4 Notes

1. The Wiesner test solution only works when using an acidified ethanolic solution of phloroglucinol or 1,3,5-benzenetriol and will not work if using pyrogallol or 1,2,3-benzenetriol. Note that protecting the solution from light with aluminum foil will decrease the yellowing of the solution with time.
2. Enzyme used for making DHP is not limited to peroxidase and, other phenoloxidase such as laccase can be used [15].
3. Other organic solvents can be used for the solubilisation of phenylpropanoid monomer, such as acetone:phosphate buffer [16].
4. When using laccase enzymes, either air bubbling should be used to increase oxygenation instead of dripping a solution H_2O_2 or adding catalase to the enzyme solution to release O_2 from the breaking down of H_2O_2.

5. Plumbing or Teflon sealing tape can be used to ensure that the fit between syringe needle and silicon tubing is tight (Fig. 2).
6. The freeze-drying is essential for the GC column as any residual water molecules in the sample will damage the lifetime of GC columns.
7. The uses of more beads increases friction and will burn the sample, causing both loss of materials and contaminating artefacts.
8. No readjustment for difference in the relative response factor are generally performed, although they differ quite significantly between pyrolyzates [21].
9. Distinction in thioacidolysis between internal and terminal residues with free aromatic part can be performed by permethylating lignin prior to thioacidolysis (Fig. 4). This permethylation step will change the *para* hydroxy group of terminal residues with free aromatic part into methoxy group, which can then be distinguished from internal indenes.
10. 100 °C is not the set temperature of the sand bath but the actual temperature in the sand near the sample, measured using a thermometer.
11. Put containers used for thioacidolysis in sodium hypochlorite aqueous solution for several days, and wash when there is no smell.
12. Note that calibration to "Uncalibrated OD" will inverse the scale, thus requiring the "Image/Lookup tables/invert LUT".
13. Press on "Alt" key to ensure that the line ROI does not change size when moved at different location in the image so that average profile can be measured for the same length ROIs (Fig. 10).

Acknowledgments

We thank Prof. Yasuyuki Matsushita (TUAT, Japan), Prof. Catherine Lapierre (INRA Versailles, France) and Prof. John Ralph (Univ. Wisconsin-Madison, USA) for comments and help on the chemical processes associated with thioacidolysis and its quantification. We thank Kevin Rein for help with the acid dependency of the Wiesner test. This work was supported by Vetenskapsrådet VR (grant 2010-4620 and 2016-04727), the BioImprove FORMAS (to EP), the Kempe Foundation (Gunnar Öquist Fellowship to EP), the Stiftelsen för Strategisk Forskning (ValueTree to EP), the Bolin Centre for Climate Research RA3, RA4 and RA5 "seed money" and "Engineering Mechanics for Climate Research" (to EP), and the Carl Trygger Foundation CTS 16:362/17:16/18:306/21:1201

(to EP). We also thank Bio4Energy (a strategic research environment appointed by the Swedish government), the UPSC Berzelii Centre for Forest Biotechnology, and the Departments of Materials and Environmental Chemistry (MMK), of Organic Chemistry (OK), of Ecology, Environment and Plant Sciences (DEEP), and the Bolin Centre for Climate Research of Stockholm University (SU).

References

1. Ménard D, Blaschek L, Kriechbaum K et al (2022) Plant biomechanics and resilience to environmental changes are controlled by specific lignin chemistries in each vascular cell type and morphotype. Plant Cell 34:4877–4896
2. Boerjan W, Ralph J, Baucher M (2003) Lignin biosynthesis. Ann rev. Plant Biol 54:519–546
3. Barros J, Serk H, Granlund I et al (2015) The cell biology of lignification in higher plants. Ann Bot 115:1053–1074
4. Pesquet E, Wagner A, Grabber JH (2019) Cell culture systems: invaluable tools to investigate lignin formation and cell wall properties. Curr Opin Biotechnol 56:215–222
5. Serk H, Gorzsás A, Tuominen H et al (2015) Cooperative lignification of xylem tracheary elements. Plant Signal Behav 10:e1003753
6. Blaschek L, Murozuka E, Serk H et al (2023) Different combinations of laccase paralogs nonredundantly control the amount and composition of lignin in specific cell types and cell wall layers in Arabidopsis. Plant Cell 35:889–909
7. Blaschek L, Champagne A, Dimotakis C et al (2020) Cellular and genetic regulation of coniferaldehyde incorporation in lignin of herbaceous and woody plants by quantitative Wiesner staining. Front Plant Sci 11:109
8. Peng F, Westermark U (1997) Distribution of coniferyl alcohol and coniferaldehyde groups in the cell wall of spruce fibers. Holzforschung 51:531–536
9. Kutscha NP, Gray JR (1972) The suitability of certain stains for studying lignification in balsam fir, Abies balsamea (L.). Mill Tech Bull Univ Maine 53:1–51
10. Van Acker R, Vanholme R, Storme V et al (2013) Lignin biosynthesis perturbations affect secondary cell wall composition and saccharification yield in Arabidopsis thaliana. Biotechnol Biofuels 6:46
11. Yamamoto M, Blaschek L, Subbotina E et al (2020) Importance of lignin coniferaldehyde residues for plant properties and sustainable uses. ChemSusChem 13:4400–4408
12. Holmgren A, Norgren M, Zhang L et al (2009) On the role of the monolignol gamma-carbon functionality in lignin biopolymerization. Phytochemistry 70:147–155
13. Blaschek L, Nuoendagula BZ et al (2020) Determining the genetic regulation and coordination of lignification in stem tissues of Arabidopsis using semiquantitative Raman microspectroscopy. ACS Sustain Chem Eng 8: 4900–4909
14. Méchin V, Baumberger S, Pollet B et al (2007) Peroxidase activity can dictate the in vitro lignin dehydrogenative polymer structure. Phytochemistry 4:571–579
15. Kishimoto T, Hiyama A, Toda H et al (2022) Effect of pH on the Dehydrogenative polymerization of Monolignols by laccases from Trametes versicolor and Rhus vernicifera. ACS Omega 7:9846–9852
16. Tobimatsu Y, Chen F, Nakashima J et al (2013) Coexistence but independent biosynthesis of catechyl and guaiacyl/syringyl lignin polymers in seed coats. Plant Cell 25:2587–2600
17. Kawamoto H (2017) Lignin pyrolysis reactions. J Wood Sci 63:117–132
18. Gerber L, Eliasson M, Trygg J et al (2012) Multivariate curve resolution provides a high-throughput data processing pipeline for pyrolysis-gas chromatography/mass spectrometry. J Anal Appl Pyrolysis 95:95–100
19. Faix O, Meier D (1989) Pyrolytic and hydrogenolytic degradation studies on lignocellulosics, pulps and lignins. Holz als Roh-und Werkstoff 47:67–72
20. Ralph J, Hatfield RD (1991) Pyrolysis–GC–MS characterization of forage materials. J Agric Food Chem 39:1426–1437
21. Van Erven G, de Visser R, Merkx DWH et al (2017) Quantification of lignin and its structural features in plant biomass using 13C lignin as internal standard for pyrolysis-GC-SIM-MS. Anal Chem 89:10907–10916
22. Kim H, Ralph J, Lu F et al (2002) Identification of the structure and origin of thioacidolysis marker compounds for cinnamyl alcohol

dehydrogenase deficiency in angiosperms. J Biol Chem 277:47412–47419

23. Pomar F, Merino F, Barceló AR (2002) O-4-linked coniferyl and sinapyl aldehydes in lignifying cell walls are the main targets of the Wiesner (phloroglucinol-HCl) reaction. Protoplasma 220:17–28
24. Preibisch S, Saalfeld S, Tomancak P (2009) Globally optimal stitching of tiled 3D microscopic image acquisitions. Bioinformatics 25: 1463–1465
25. Schindelin J, Arganda-Carreras I, Frise E et al (2012) Fiji: an open-source platform for biological-image analysis. Nat Methods 9: 676–682
26. Schroeder AB, Dobson ETA, Rueden CT et al (2021) The ImageJ ecosystem: open-source software for image visualization, processing, and analysis. Protein Sci 30:234–249
27. Lapierre C, Pilate G, Pollet B et al (2004) Signatures of cinnamyl alcohol dehydrogenase deficiency in poplar lignins. Phytochemistry 65(3):313–321
28. Ito T, Kawai S, Ohashi S et al (2002) Characterization of new thioacidolysis products of sinapyl aldehyde and coniferyl aldehyde. J Wood Sci 48:409–413